Chemically Fueled Reinforcement of Polymer Hydrogels

Chamoni W. H. Rajawasam,^a Corvo Tran,^a Michael Weeks,^b Kathleen S. McCoy,^c Robert Ross-Shannon,^c Obed J. Dodo,^a Jessica L. Sparks,^c C. Scott Hartley,^{a,*} and Dominik Konkolewicz^{a,*}

- a. Miami University Department of Chemistry and Biochemistry, Oxford, OH, 45056, USA.
- b. Miami University Instrumentation Laboratory, Oxford, OH, 45056, USA.
- c. Miami University Department of Chemical Paper and Biomedical Engineering, Miami University, Oxford, OH, 45056 USA.

ABSTRACT: Carbodiimide-fueled anhydride bond formation has been used to enhance the mechanical properties of permanently crosslinked polymer networks, giving materials that exhibit transitions from soft gels to covalently reinforced gels, eventually returning to the original soft gels. Temporary changes in mechanical properties result from a transient network of anhydride crosslinks which eventually dissipate by hydrolysis. Over an order of magnitude increase in storage modulus is possible through carbodiimide fueling. The time-dependent mechanical properties can be modulated by the concentration of carbodiimide, temperature, and primary chain architecture. Because the materials remain rheological solids, new material functions such as temporally controlled adhesion and rewritable spatial patterns of mechanical properties have been realized.

INTRODUCTION

Biology commonly uses chemical reactions, such as ATP and GTP hydrolysis, to drive chemical systems out of equilibrium.1,2 The results are time-dependent behavior dictated by kinetics and dynamic properties.³ Following pioneering work by Van Esch and Eelkema,4 recent work focuses on using chemical "fuels" in non-biological contexts, with reports of responsive supramolecular structures,5-7 self-healing systems,8 and adaptive materials.9-11 Applying fuels to polymer materials is a useful first step toward practical applications of these nonequilibrium systems. We recently showed that the carbodiimidedriven formation of anhydrides, developed concurrently by Boekhoven and our group, 12,13 can be used to generate temporary crosslinks in polymer systems;14,15 similar materials have since been adapted by Wang for potential medical applications.¹⁶ Walther has used carbodiimide chemistry to induce phase separation by increasing the hydrophobicity of polyacid microgels,¹⁷ and has studied timedependent phase separation of poly(norbornene dicarboxylic acid).18 Wang has introduced a writable and selferasable hydrogel through transient polymerization of tetrafunctional monomers.19

Most temporally controlled polymer systems to this point use the fuel to achieve transient phase changes (e.g., sol \rightarrow gel \rightarrow sol). In many materials applications, however, more subtle behavior is needed, with transient changes in mechanical properties while maintaining the material's structural integrity. In a recent publication, Eelkema showed that temporary cationic charges could be introduced in polymer networks through quaterniza-

tion of amine-containing monomers.²⁰ This process alters the interactions between the polymer and solvent, leading to controlled hydrogel swelling. However, this does not change the net crosslink density that holds the network together, which is integral to mechanical properties. Further, in a recent paper, the carbodiimide 1-ethyl-3-(3-dimethylaminopropyl)carbodiimide (EDC) was used to actuate a polydimethylsiloxane network by forming temporary anhydride bonds.²¹ Substantial and controlled shape change was possible by this approach, but the modulation of mechanical and adhesive properties was not realized.

Here, we report that a permanently crosslinked polymer network with pendent carboxylic acid groups can temporarily increase its modulus by the formation of transient crosslinks upon addition of EDC. The EDCdriven anhydride bond formation, with subsequent hydrolysis to return to the resting state, is used as a model system to highlight new capabilities arising from fully gelbased transitions. The materials display transitions from soft gels to covalently reinforced gels which eventually return to the original soft gels. That is, the materials are rheological solids in both the fueled and the resting states, defined as systems with storage modulus (G') greater than the loss modulus (G"), or, equivalently, tan δ < 1 ($\delta = G''/G'$). The impacts of network architecture, including chain length, crosslink density, and the extrinsic parameters of temperature and EDC concentration, on the transient properties of the material have been investigated. Because the materials remain rheological solids throughout the fueling, new functional properties of the transient polymer networks have been realized. First, two hydrogels can be repeatedly adhered by the addition of EDC. Second, spatial control over where EDC is applied¹⁹ enables temporary 2D patterned mechanical properties in a hydrogel film, which can subsequently be transformed into new designs.

RESULTS AND DISCUSSION

The initial polymer networks were synthesized by reversible addition-fragmentation chain transfer (RAFT) polymerization, as shown in Scheme 1a.²² Monomers included acrylic acid (AA) as the active carboxylic-acid-containing monomer that can be transiently crosslinked, acrylamide (Am) as an inert backbone-forming monomer, and *N*,*N*'-methylene bisacryalamide (MBAm) as a perma-

2-(((Ethylthio)nent covalent crosslinker. carbonothioyl)thio) propionic acid (PAETC) was used as the chain transfer agent (CTA) and 2,2'-azobis[2-(2imidazolin-2-yl)propane]dihydrochloride (VA-044) as the radical initiator. The networks were synthesized with either 100 or 200 total monomer units in the primary chain; 15%, 30%, or 50% AA; and either 1.3% or 1.6% MBAm (1.3% MBAm per primary chain was the lowest that led to reliable gelation). The fraction of AA impacts the maximum density of transient crosslinks that result from EDC fueling, while the proportion of MBAm controls the permanent crosslink density. The polymer materials are denoted as poly(Am_x - AA_y - $MBAm_z$) where x, y, and z represent the total number of repeating units of AA, Am and MBAm in the primary chain.

Scheme 1. (a) Polymer synthesis. (b) Overview of carbodiimide-induced crosslinking.

The overall concept is shown in Scheme 1b. In these polymer networks, the crosslink density should increase through the formation of temporary anhydrides after EDC fueling. The systems then should return to the resting state through hydrolysis. Polymer hydrogels were prepared at 33 wt% polymer in water. For all rheological time sweep experiments, 20 mm diameter disc-shaped materials were used with thickness of ~1 mm. EDC was delivered to the hydrogel by placing a solution on top of the hydrogel material and allowing mixing by the rheometer action.

As shown in Figure 1a, immediately after adding EDC to a hydrogel of poly(Am_{70} - AA_{30} - $MBAm_{1.3}$) there was a rapid increase in G, reaching a peak within ~60 min. The material then relaxed to its original state over the course of hours. Control experiments, labelled "blank", showed that adding water without EDC yields no significant change in

mechanical properties. Higher concentrations of EDC led to larger *G'* values (Figure 1a).

The behavior could be repeated with an additional cycle of EDC (Figure S1): following treatment of a poly(Am_{70} - AA_{30} - $MBAm_{1,3}$) sample with 2.0 M EDC, which gave the expected rise and fall of G, a subsequent addition of 2.0 M EDC restored the modulus to its peak, with the material again returning to its softer state. At least over this second cycle the performance of the system did not significantly degrade. While the buildup of the urea byproduct must eventually degrade the properties of the system, ²³ previous transient gels based on crosslinked polymers were resistant to the urea over many cycles. ^{14,15}

The previously established behavior of Am/AA copolymers and the timescales of the experiments are consistent with the formation of temporary anhydride crosslinks

(Scheme 1b). ^{14,15} After consumption of EDC, the anhydride linkers eventually hydrolyze, returning the material to the original state. In network solids, the total crosslink density, from both permanent and transient crosslinks, is proportional to G'. ^{24,25} Therefore, the presence of transient anhydride crosslinkers in the polymer causes G' to be higher than the initial G', or that of the material treated only with water. The peak storage modulus (G'_{max}) of a given system thus corresponds to the maximum crosslink density. As the anhydride crosslinks hydrolyze, the G' decreases and levels off, consistent with the unfueled system.

Figure 1b shows that all materials remain rheological solids, with tan δ < 1, at all times. This is in contrast to other systems which transition from rheological liquids to solids and back. Therefore, this EDC fueled system transiently changes its mechanical properties, while remaining in the solid state. Note that tan δ is plotted on a linear y-axis scale, making small differences in the ratio of G" to G' more apparent. This is distinct from the moduli, G', which are plotted on a logarithmic y-axis scale. There is evidence of a small increase in tan δ during fueling, especially at higher EDC loadings, in Figure 1b. This could be due to some bond exchange between anhydrides and free carboxylic acids, increasing G".

As the discs contained 33 wt% polymer, corresponding to 0.28 g of polymer, the addition of 0.1 mL of 0.5 M EDC corresponds to a ratio of carboxylic acid to EDC of ~1.0:0.042, while the addition of 0.1 mL of 2.0 M EDC corresponds to a ratio of carboxylic acid to EDC of ~1.0:0.17. Thus, in all cases EDC is the limiting reagent. However, because the EDC solution is applied on top of the network, it is likely that there is, at least initially, a gradient of crosslink density across the material. The inhomogeneity of the material should decrease over time as the EDC diffuses farther into the gel. It is also possible that the anhydride crosslinks themselves move deeper into the material through anhydride exchange, which is typically faster than hydrolysis.²⁶

Figure 1c shows how the EDC concentration affects both G'_{max} and, to a lesser extent, the transient network lifetime (t_{tnl}), defined here as the time needed to dissipate 90 percent of the transient crosslinkers. ²⁷ In the presence of the most concentrated EDC solution (2.00 M), G'_{max} increases to ~140 kPa, over an order of magnitude higher than the baseline storage modulus of ~10 kPa. Lower EDC concentrations lead to lower G'_{max} values, as expected, with an exponential-like dependence of G'_{max} on the EDC concentration (Figure 1c). G'_{max} can be empirically fitted with the function $G'_{max} = 12.3e^{1.13[\text{EDC}]}$ (Figure S2).

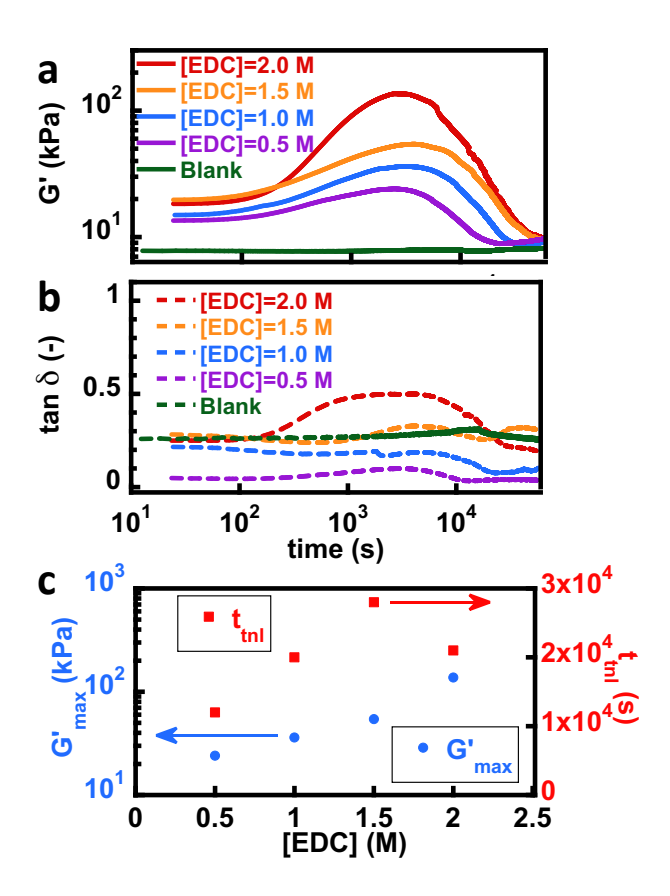


Figure 1. Impact of EDC loading on rheological time sweep of poly(Am₇₀-AA₃₀-MBAm_{1.3}) hydrogels (33 wt% polymer) at 4 °C (a) G′, (b) tan δ , and (c) G′_{max} and t_{tnl} of poly(AM₇₀-AA₃₀-MBAm_{1.3}) vs EDC concentration. All time sweep experiments were performed at 1% applied strain at a frequency of 10 rad/s. In all cases 0.1 mL of EDC solution was added.

The transient network lifetime t_{tnl} is primarily dictated by the rate of hydrolysis of the anhydride crosslinkers, especially in a well percolated network. ¹⁵Anhydride bond hydrolysis is pseudo first-order in the anhydride concentration, under ideal conditions, 15 suggesting that the t_{tnl} should not have a strong dependence on the EDC concentration. Figure 1c indicates that t_{tnl} shows an initial increase in $t_{\rm tnl}$ with EDC concentration. Eventually $t_{\rm tnl}$ reaches a peak or plateau above an EDC concentration of 1 M. At high EDC concentrations, a strongly percolated network of anhydrides is expected. Under these conditions, pseudo-first-order decay kinetics of the anhydrides could be anticipated, leading to similar network lifetimes regardless of the EDC concentration (since t_{tnl} is defined in terms of the maximum *G*' and thus crosslink density).¹⁵ However, at lower EDC concentrations, the anhydride network percolation should be relatively poor, leading to poor network formation, and relatively fewer hydrolyses are needed to return the system to the resting state. That said, other complex non-linear behavior in t_{tnl} with EDC loading cannot be ruled out.

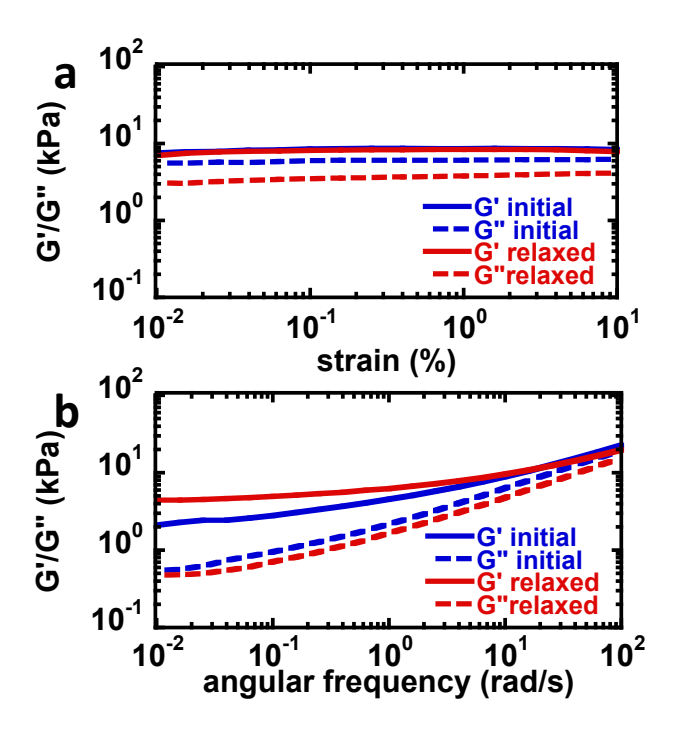


Figure 2. (a) Strain sweep of poly(Am_{70} - AA_{30} - $MBAm_{1.3}$) hydrogel (33 wt% polymer) at 4 °C using a frequency of 10 rad/s initially and in the relaxed state after fueling. (b) Frequency sweep of poly(Am_{70} - AA_{30} - $MBAm_{1.3}$) hydrogel (33 wt% polymer) at 4 °C using a strain of 1% initially and in the relaxed state after fueling. The relaxed state is achieved by waiting 16 h and 4 °C after the addition of EDC.

To confirm that the material returns to a state similar to the initial one, strain and frequency sweeps were performed on the poly(Am₇₀-AA₃₀-MBAm_{1.3}) hydrogel materials before and after fueling. The after-fueling, or relaxed, state was achieved by waiting 18 h after the addition of EDC at 4 °C. As indicated in Figure 2, there was no substantial difference in material between the initial and the relaxed state after the EDC was fully consumed. The small differences in the moduli could be due to a small amount of evaporation of the water solvent between the measurements, or the presence of the urea byproduct. Nevertheless, the materials properties are substantively unchanged by the fueling chemistry. The data in Figure 2a indicate that linear viscoelasticity is observed, independent of applied strain over several orders of magnitude. Figure 2b suggests that a rubber like plateau in modulus is achieved below an angular frequency of ~10 rad/s.

Since the fueled state of these materials contains both permanent MBAm and transient anhydride crosslinkers, the impact of the permanent crosslink density was probed. When the MBAm:PAETC ratio was increased to 1.6:1, the response to fueling was smaller (compare Figures 1 and S₃), with a lower G'_{max} with the higher ratio of MBAm. The resting states of the materials were typically in the order of 8-13 kPa, indicating that the substantially higher G'_{max} possible for the lower MBAm ratio at lower temperatures was due to more-efficient transient anhydride bond formation, rather than substantial changes in the resting state. The higher G'_{max} with lower MBAm load-

ing is attributed to the higher density of permanent MBAm crosslinks hindering chain mobility, inhibiting the formation of transient anhydride bonds. Specifically, a higher density of permanent MBAm-based crosslinkers tethers the polymer chains to more points in the network, restricting the ability of the carboxylic acids on two distinct primary chains from diffusing near each other and forming an anhydride bond during the fueling process.

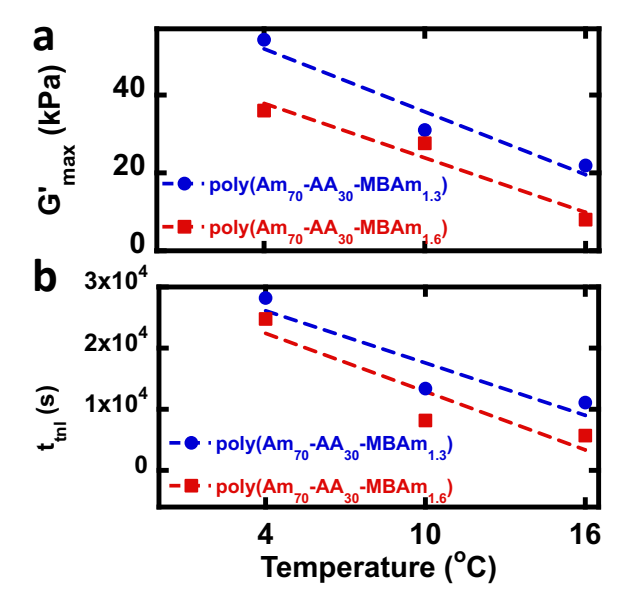


Figure 3. Rheological data of poly(Am_{70} - AA_{30} - $MBAm_{1.6}$) & poly(Am_{70} - AA_{30} - $MBAm_{1.3}$) adding 0.2 mL of 1.50 M EDC. a) G'_{max} and b) t_{tnl} as a function of temperature for each network. All time sweep experiments were performed at 1% applied strain at a frequency of 10 rad/s.

The impact of temperature was also considered, at 4 °C, 10 °C, and 16 °C, shown in Figure 3. The highest G'_{max} and longest t_{tnl} values were observed at 4 °C. At low temperatures, the hydrolysis rate decreases, extending the lifetime of the network and allowing a higher temporary crosslink density to build up from the EDC fuel. Although larger G'_{max} values are observed at temperatures near o °C, where retardation of anhydride hydrolysis occurs, the system still functions at higher temperatures as demonstrated in Figure 3. The ability to control the hydrolysis lifetimes, and thereby impact the transient lifetime of the material is confirmed by an experiment where the temperature was maintained at 4 °C for 10,000 s followed by an increase to 16 °C (Figure S4). The G' decreased rapidly after the increase in temperature.

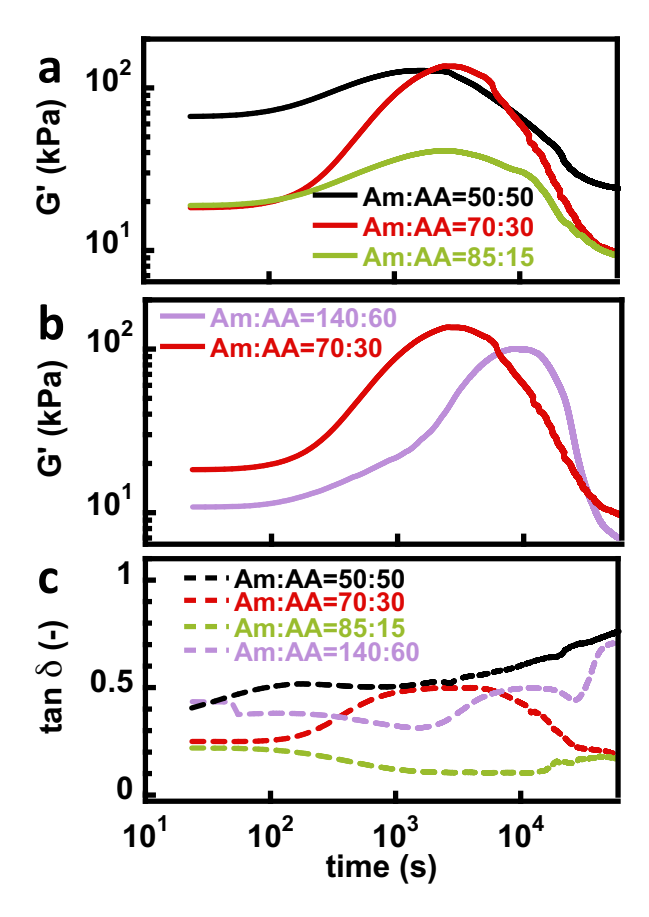


Figure 4. (a) Rheological time sweeps of poly(Am₈₅-AA₁₅-MBAm_{1.3}), poly(Am₇₀-AA₃₀-MBAm_{1.3}), and poly(Am₅₀-AA₅₀-MBAm_{1.3}) hydrogels (33 wt% polymer) at 4 °C adding 0.1 mL of 2.00 M EDC. (b) Rheological time sweeps of poly(Am₇₀-AA₃₀-MBAm_{1.3}) and poly(Am₁₄₀-AA₆₀-MBAm_{1.3}) at 4 °C using 2.00 M EDC. (c) The associated tan δ for all five materials. All time sweep experiments were performed at 1% applied strain at a frequency of 10 rad/s.

The impact of polymer architecture on material properties was also explored. Initially, the Am to AA ratio was varied, using primary chain compositions of poly(Am₅₀- AA_{50} - $MBAm_{1.3}$), $poly(Am_{70}-AA_{30}-MBAm_{1.3}),$ poly(Am₈₅-AA₁₅-MBAm_{1.3}), maintaining the total primary chain length of 100 units. As seen in Figure 4a, poly(Am₅₀ -AA₅₀-MBAm_{1.3}) had the highest *G'max* and longest transient network lifetime, while poly(Am₈₅-AA₁₅-MBAm_{1.3}) had the lowest G'max and shortest transient network lifetime; however, all networks had transient network lifetimes on the order of 20,000 s. A similar trend of increased G'_{max} with higher AA density was observed in previous studies^{14,15} that focused on EDC-fueled sol-gel-sol transitions. The G'max values were similar for poly(Am₅₀-AA₅₀-MBAm_{1.3}) and poly(Am₇₀-AA₃₀-MBAm_{1.3}). This small difference is in part due to the EDC acting as a limiting reagent, even at 2.00 M: since the hydrogel was 33wt% polymer, giving 0.28 g of polymer, the addition of 0.1 mL of 2.0 M EDC corresponds to a ratio of carboxylic acid to EDC of ~1.0:0.33 for poly(Am₈₅-AA₁₅-MBAm_{1.3}), carboxylic acid to EDC of ~1.0:0.17 for poly(Am₇₀-AA₃₀-MBAm_{1.3}), and carboxylic acid to EDC of ~1.0:0.10 for poly(Am₅₀-AA₅₀-

MBAm_{1.3}). A possible reason for the poly(Am₈₅-AA₁₅-MBAm_{1.3}) having a lower modulus is that with the lower density of AA units, intramolecular crosslinking could be more difficult with the chains not being able to diffuse near each other within the hydrogel, potentially facilitating elastically ineffective intramolecular loops.

Using the same volume of a 3.00 M EDC solution causes G'_{max} to reach over 0.70 MPa for poly(Am₅₀-AA₅₀-MBAm_{1.3}) (Figure S₅). Surprisingly, this led to higher tan δ values, in some cases having tan δ ~ 1 or even tan δ > 1 during the time sweep. The higher G' when using 3.0 M EDC, compared to 2.0 M EDC, suggests that more anhydride crosslinks are formed with the higher EDC loading. Therefore, a likely explanation for the higher G' concurrent with higher G' when using 3.0 M EDC is the exchange of the anhydride linkers, ²⁶ leading to more viscous properties. In prior work, higher densities of anhydride linkers did lead to increase in both G' and G''. ¹⁵

In addition to composition, chain length effects were explored using poly(Am₇₀-AA₃₀-MBAm_{1.3}) and poly(Am₁₄₀-AA₆₀-MBAm_{1.3}). A small difference of ~40 kPa between the G'_{max} values of two the polymers shows that chain length has minimal impact. However, Figure 4b indicates that poly(Am₇₀ -AA₃₀-MBAm_{1.3}) forms temporary crosslinks much faster than poly(Am₁₄₀-AA₆₀-MBAm_{1,3}). Since longer chains have lower diffusion rates, this can cause both a delay in the peak but also a higher t_{tnl} . Since the small molecule EDC has a substantially lower molecular weight than the polymer chains, it is not expected to have similar diffusion rates in both poly(Am₇₀-AA₃₀-MBAm_{1.3}) and poly(Am₁₄₀-AA₆₀-MBAm_{1.3}). This suggests that the changes in the network diffusion processes and mobility are primarily responsible for the changes in G' and network lifetimes at the different chain lengths studied. This phenomenon can be clearly observed in the decay profile of G'. These results suggest that t_{tnl} can be modulated strongly using primary chain length while maintaining a near constant G'_{max} . As longer chains are used, the chain mobility diminishes, reducing the likelihood of forming elastically effective anhydride crosslinkers in a given timeframe. The reduction in chain mobility becomes more significant as the anhydride crosslink density increases. This could lead to an extended transient network lifetime by increasing the time needed to reach the peak of G' and extending the time spent near the peak in *G*′ as indicated in Figure 4b.

Figure 4c shows that all polymer compositions and chain lengths remained rheological solids throughout the experiments. However, it also indicates that the tan δ profiles differ between the materials. In particular, the materials with longer chain lengths, poly(Am₁₄₀-AA₆₀-MBAm_{1.3}), or the highest amount of pendant carboxylic acid, poly(Am₅₀-AA₅₀-MBAm_{1.3}), had higher tan δ values, particularly in the resting state. This could be due to energy dissipation through hydrogen bonds, short lived entanglements, and other non-covalent interactions, which are suppressed in the transiently crosslinked state. This is because higher G" values, and consequently higher tan δ , could also result from covalent or non-covalent bond ex-

change. ^{28,29} As noted above, the poly(Am_{50} - AA_{50} - $MBAm_{1,3}$) material fueled with 3.0 M EDC showed a higher tan δ with $G'' \sim G'$ (Figure S5). This is consistent with the EDC-fueled behavior observed in sol-gel-sol transitions, where higher pendant carboxylic acid concentrations led to lower tan δ . ¹⁴ This could be due to the higher ratio of carboxylic acid leading to more exchange of free acids and anhydrides.

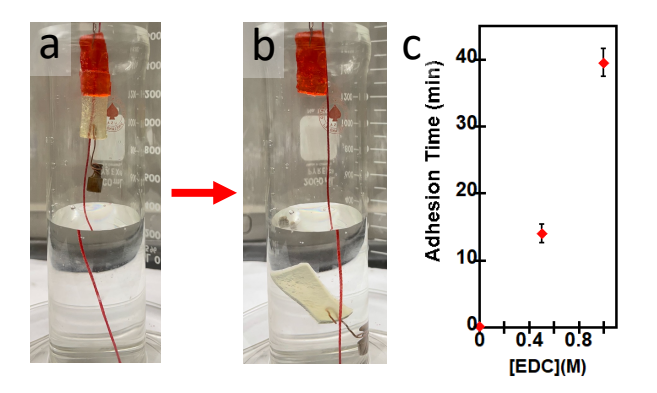


Figure 5. (a) Adhesion of hydrogel pieces holding a 2 g weight. (b) Failure of adhesive after ~40 min following treatment with 1 M EDC solution. (c) Time taken for the adhesive to fail vs EDC concentration, based on duplicate experiments. Error bars represent the standard deviation.

The developed hydrogel materials exhibit new behavior not previously demonstrated for chemically fueled systems. For example, two acid-containing hydrogels can be temporarily adhered by treating their surfaces with EDC. As shown in Figure 5a, two pieces of poly(Am₇₀-AA₃₀-MBAm_{1,2}) (colored so that they can be distinguished) were adhered by applying EDC solutions (0.1 mL) over a 1 cm² interface. The materials were hung and held a 0.02 N force, applied by attaching 2 g weight to the bottom piece. Eventually, the anhydride bonds dissipated through hydrolysis and the adhesive failed as seen in Figure 5b. The efficiency of this EDC fueled adhesion was quantified by time needed for the pieces to separate. When treated with only water, the two hydrogel pieces detached within 6 s. In contrast, with 1 M EDC the two pieces of hydrogel remained adhered for ~40 min, an almost 400-fold increase, as shown in Figure 5c. Repeated adhesion was possible by refueling with fresh EDC (Table S2).

Patterned hydrogels are of current interest, particularly for biological applications.^{30,31} Spatial patterning has been achieved by using, for example, light^{32,33} or printing.^{34,35} With the new hydrogels, it is possible to use EDC solutions to produce a rewriteable pattern of distinct mechanical properties. Masks were designed that prevent EDC ingress into targeted regions, as shown in Figure 6a. The EDC was deposited onto the surface of the exposed film as a mist using a spray bottle, delivering 2.0 mL of 2.0 M EDC. The masks prevent EDC reaching covered regions of the hydrogel. Additionally, the EDC served as the limiting reagent, implying that EDC is more likely to react with carboxylic acids in the region where they EDC is sprayed rather than diffusing beyond the masked region.

A representative example used a square poly(Am_{70} - AA_{30} - $MBAm_{1.3}$) polymer film (5 × 5 × 1.5 cm). The stiffness of the material was probed in a 6 × 6 indentation grid using a robotic indenter. This indenter can raster across the surface of the material, yielding a shear modulus (G) at each location. The shear modulus is related to the indentation depth (i) and measured peak force (F_{peak}) using the spherical indenter of radius (r) using the relationship developed by Lee and Radok for indentation of an elastic half-space: 36

$$G = \frac{{}_{3}F_{peak}}{{}_{16i\sqrt{r\,i}}}\tag{1}$$

Prior to EDC treatment, all G values were on the order of 9-18 kPa, with no discernable pattern, as shown in Figure 6c (left). This is consistent with the shear modulus evaluated by rheology for the unfueled materials given in Figure 1. While shear modulus, G, is a quasi-static material property defined by the ratio of shear stress to shear strain, rheological moduli G' and G'' are dynamic in nature and are not expected to be identical numerically to G values obtained via indentation experiments. Nevertheless, both the shear modulus G and the storage modulus G' may be interpreted as measures of the resistance to deformation of the material in shear loading (i.e. how much energy must be applied to a sample in order to distort it), so comparing G and G' results qualitatively can be informative.

The hydrogel was then subjected to a series of treatments with EDC, shown in Figure 6b. First, a 3 × 3 checkerboard mask was used. The resulting pattern of *G* values after spraying with 2.0 mL of 2.0 M EDC solution was completely consistent with the pattern of the mask. The regions that were not exposed to EDC remain essentially unchanged, with *G* increasing slightly to 13–18 kPa. This is similar to the shear modulus of the blank samples of the time sweep rheological experiments in Figure 1. In contrast, the regions that were exposed to EDC have *G* values in the range 21-33 kPa. The increase in modulus is somewhat smaller than the peak modulus in time sweep rheology experiment using 2.0 M EDC sample in Figure 1, most likely because of the substantially thicker hydrogel used in the indentation experiments (1.5 cm), compared to the thickness of the samples used in the rheological studies, which was on the order of 1-2 mm. This higher thickness effectively dilutes the EDC within the network. Nevertheless the trend is consistent with the data in Figure 1.

Since the anhydride crosslinkers are subject to hydrolysis, 7 h after adding the EDC the material returns to the resting state of patternless *G* values in the range of 9–20 kPa, again consistent with the time sweep rheological experiment of the blank sample in Figure 1. A mask of the letter "M" was then used to pattern the film. The new regions exposed to EDC again achieved *G* values in the range of 21–28 kPa while non-EDC areas were in the range of 9–20 kPa, consistent with the mask. These trends are again similar to the fueled and blank time sweep rheological studies of Figure 1, except again the magnitude of the increase in modulus for the system fueled with 2.0 M EDC was somewhat smaller in the indentation experiment

than in the time sweep. This is again most likely due to the thicker sample used in the indentation experiment effectively diluting the EDC. After allowing the anhydride bonds to hydrolyze over 7 h, the material returned to the resting state with *G* values of 10-19 kPa with no discernable pattern. As expected, the shear moduli of the resting state were consistent with the unfueled system studied by rheology in Figure 1.

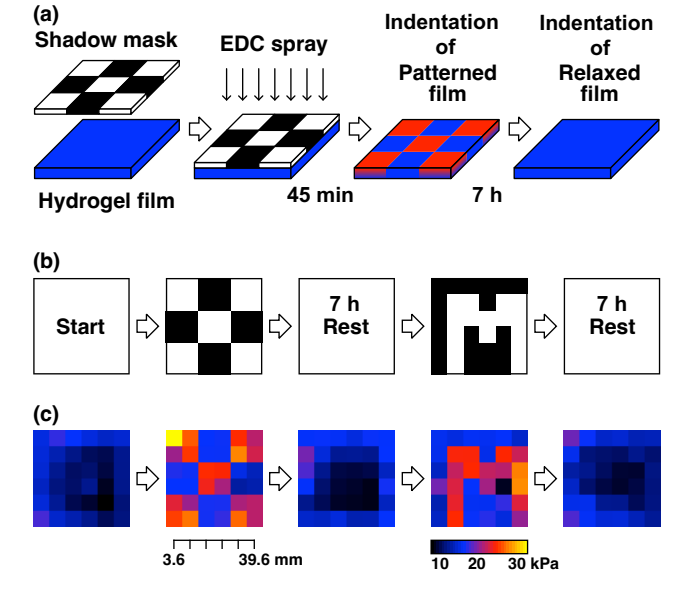


Figure 6. (a) Mask based patterning of hydrogel films with EDC. (b) Sequence of events for rewritable patterning of a poly(Am_{70} - AA_{30} - $MBAM_{1.3}$) film. In the mask images, dark areas block the EDC spray. (c) Experimental G readings at regular points on the sprayed hydrogel of dimensions $5\times5\times1.5$ cm. Indentation was performed on a 6×6 pattern. Indentation was performed 45 min after fueling, and again after 7 h of rest.

CONCLUSIONS

In conclusion, EDC-driven anhydride formation has been used to achieve transient changes in the mechanical properties of hydrogels with pendent carboxylic acid groups. The strength of the effect was modulated by changing polymer architecture and external factors including temperature and EDC concentration, with up to an order of magnitude increase in *G*'. As these are rheological solid materials at all times, new material properties and functions are possible, including temporary repeatable adhesion and spatial patterning of mechanical properties.

ASSOCIATED CONTENT

Supporting Information

The Supporting Information is available free of charge on the ACS Publications website.

Experimental details and supplemental data (PDF)

AUTHOR INFORMATION

Corresponding Author

- * CSH (scott.hartley@miamiOH.edu)
- * DK (d.konkolewicz@miamiOH.edu)

Author Contributions

The manuscript was written through contributions of all authors. All authors have given approval to the final version of the manuscript.

Funding Sources

This work was supported by United States Department of Energy, Office of Science, Basic Energy Sciences, under Award No. DE-SC0018645 for network synthesis and characterization. 400 MHz NMR instrumentation at Miami University is supported through funding from the National Science Foundation under Award No. CHE-1919850.

ACKNOWLEDGMENT

The authors thank Miami University for supporting the Instrumentation Laboratory.

REFERENCES

- (1) Dogterom, M.; Koenderink, G. H. Actin-Microtubule Crosstalk in Cell Biology. *Nat Rev Mol Cell Biol* **2019**, *20* (1), 38–54. https://doi.org/10.1038/s41580-018-0067-1.
- (2) Das, K.; Gabrielli, L.; Prins, L. J. Chemically Fueled Self-Assembly in Biology and Chemistry. *Angewandte Chemie International Edition* **2021**, *60* (37), 20120–20143. https://doi.org/10.1002/anie.202100274.
- (3) Kariyawasam, L. S.; Hossain, M. M.; Hartley, C. S. The Transient Covalent Bond in Abiotic Nonequilibrium Systems. *Angewandte Chemie International Edition* **2021**, *60* (23), 12648–12658. https://doi.org/10.1002/anie.202014678.
- (4) Boekhoven, J.; Hendriksen, W. E.; Koper, G. J. M.; Eelkema, R.; van Esch, J. H. Transient Assembly of Active Materials Fueled by a Chemical Reaction. *Science* (1979) 2015, 349 (6252), 1075–1079. https://doi.org/10.1126/science.aac6103.
- (5) van Rossum, S. A. P.; Tena-Solsona, M.; van Esch, J. H.; Eelkema, R.; Boekhoven, J. Dissipative Out-of-Equilibrium Assembly of Man-Made Supramolecular Materials. *Chem Soc Rev* **2017**, *46* (18), 5519–5535. https://doi.org/10.1039/c7cs00246g.
- (6) Das, K.; Chen, R.; Chandrabhas, S.; Gabrielli, L.; Prins, L. J. Design of Chemical Fuel-Driven Self-Assembly Processes. In *Out-of-Equilibrium (Su-pra)molecular Systems and Materials*; Wiley, 2021; pp 191–213. https://doi.org/10.1002/9783527821990.ch7.
- (7) Sorrenti, A.; Leira-Iglesias, J.; Markvoort, A. J.; de Greef, T. F. A.; Hermans, T. M. Non-Equilibrium Supramolecular Polymerization. *Chem Soc Rev* **2017**, *46* (18), 5476–5490. https://doi.org/10.1039/c7cs00121e.
- (8) Li, P.; Hao, J.; Wang, X. Systems Chemistry in Self-Healing Materials. *ChemSystemsChem* **2021**, 3 (5), e2100016. https://doi.org/10.1002/syst.202100016.
- (9) van Ravensteijn, B. G. P.; Voets, I. K.; Kegel, W. K.; Eelkema, R. Out-of-Equilibrium Colloidal Assembly Driven by Chemical Reaction Networks. *Langmuir* **2020**, 36 (36), 10639–10656. https://doi.org/10.1021/acs.langmuir.oco1763.
- (10) van Ravensteijn, B. G. P.; Hendriksen, W. E.; Eelkema, R.; van Esch, J. H.; Kegel, W. K. Fuel-Mediated Transient Clustering of Colloidal Building Blocks. *J Am*

- *Chem Soc* **2017**, *139* (29), 9763–9766. https://doi.org/10.1021/jacs.7b03263.
- (11) Olivieri, E.; Quintard, G.; Naubron, J. V.; Quintard, A. Chemically Fueled Three-State Chiroptical Switching Supramolecular Gel with Temporal Control. *J Am Chem Soc* **2021**, *143* (32), 12650–12657. https://doi.org/10.1021/jacs.1c05183.
- (12) Kariyawasam, L. S.; Hartley, C. S. Dissipative Assembly of Aqueous Carboxylic Acid Anhydrides Fueled by Carbodiimides. *J Am Chem Soc* **2017**, *139* (34), 11949–11955. https://doi.org/10.1021/jacs.7b06099.
- (13) Tena-Solsona, M.; Rieß, B.; Grötsch, R. K.; Löhrer, F. C.; Wanzke, C.; Käsdorf, B.; Bausch, A. R.; Müller-Buschbaum, P.; Lieleg, O.; Boekhoven, J. Non-Equilibrium Dissipative Supramolecular Materials with a Tunable Lifetime. *Nat Commun* **2017**, *8*, 15895. https://doi.org/10.1038/ncomms15895.
- (14) Dodo, O. J.; Petit, L.; Rajawasam, C. W. H.; Hartley, C. S.; Konkolewicz, D. Tailoring Lifetimes and Properties of Carbodiimide-Fueled Covalently Cross-Linked Polymer Networks. *Macromolecules* **2021**, *54* (21), 9860–9867. https://doi.org/10.1021/acs.macromol.1c01586.
- (15) Zhang, B.; Jayalath, I. M.; Ke, J.; Sparks, J. L.; Hartley, C. S.; Konkolewicz, D. Chemically Fueled Covalent Crosslinking of Polymer Materials. *Chemical Communications* **2019**, 55 (14), 2086–2089. https://doi.org/10.1039/c8cc09823a.
- (16) Bai, S.; Niu, X.; Wang, H.; Wei, L.; Liu, L.; Liu, X.; Eelkema, R.; Guo, X.; van Esch, J. H.; Wang, Y. Chemical Reaction Powered Transient Polymer Hydrogels for Controlled Formation and Free Release of Pharmaceutical Crystals. *Chemical Engineering Journal* **2021**, 414, 128877. https://doi.org/10.1016/j.cej.2021.128877.
- (17) Heckel, J.; Loescher, S.; Mathers, R. T.; Walther, A. Chemically Fueled Volume Phase Transition of Polyacid Microgels. *Angewandte Chemie International Edition* **2021**, 60 (13), 7117–7125. https://doi.org/10.1002/anie.202014417.
- (18) Heckel, J.; Batti, F.; Mathers, R. T.; Walther, A. Spinodal Decomposition of Chemically Fueled Polymer Solutions. *Soft Matter* **2021**, *17* (21), 5401–5409. https://doi.org/10.1039/dismoo515d.
- (19) Cheng, M.; Qian, C.; Ding, Y.; Chen, Y.; Xiao, T.; Lu, X.; Jiang, J.; Wang, L. Writable and Self-Erasable Hydrogel Based on Dissipative Assembly Process from Multiple Carboxyl Tetraphenylethylene Derivative. *ACS Mater Lett* **2020**, 2 (4), 425–429. https://doi.org/10.1021/acsmaterialslett.9b00509.
- (20) Klemm, B.; Lewis, R. W.; Piergentili, I.; Eelkema, R. Temporally Programmed Polymer Solvent Interactions Using a Chemical Reaction Network. *Nat Commun* **2022**, *13* (1), 6242. https://doi.org/10.1038/s41467-022-33810-y.
- (21) Xu, H.; Bai, S.; Gu, G.; Gao, Y.; Sun, X.; Guo, X.; Xuan, F.; Wang, Y. Bioinspired Self-Resettable Hydrogel Actuators Powered by a Chemical Fuel. *ACS Appl Mater Interfaces* **2022**, *14* (38), 43825–43832. https://doi.org/10.1021/acsami.2c13368.
- (22) Perrier, S. 50th Anniversary Perspective: RAFT Polymerization A User Guide. *Macromolecules* **2017**, 50 (19), 7433-7447. https://doi.org/10.1021/acs.macromol.7b00767.
- (23) Rodon-Fores, J.; Würbser, M. A.; Kretschmer, M.; Rieß, B.; Bergmann, A. M.; Lieleg, O.; Boekhoven, J. A Chemically Fueled Supramolecular Glue for Self-

- Healing Gels. *Chem Sci* **2022**, *13* (38), 11411–11421. https://doi.org/10.1039/D2SC03691F.
- (24) Treloar, L. R. G. The Elasticity and Related Properties of Rubbers. *Reports on Progress in Physics* **1973**, *36* (7), 755–826. https://doi.org/10.1088/0034-4885/36/7/001.
- (25) Bennett, C.; Hayes, P. J.; Thrasher, C. J.; Chakma, P.; Wanasinghe, S. v.; Zhang, B.; Petit, L. M.; Varshney, V.; Nepal, D.; Sarvestani, A.; Picu, C. R.; Sparks, J. L.; Zanjani, M. B.; Konkolewicz, D. Modeling Approach to Capture Hyperelasticity and Temporary Bonds in Soft Polymer Networks. *Macromolecules* 2021, 55, 3573–3587. https://doi.org/10.1021/acs.macromol.1c02319.
- (26) Bunton, C. A.; Fuller, N. A.; Perry, S. G.; Shiner, V. J. The Pyridine Catalysed Hydrolysis of Carboxylic Anhydrides. *Tetrahedron Lett* **1961**, 2 (14), 458–460. https://doi.org/10.1016/S0040-4039(00)71753-9.
- (27). E. $G'(Ttnl) = G'plat + o.1 \times (G'max-G'plat)$, Where G'plat Is the Plateau Modulus Which Occurs after Essentially All Anhydrides Are Hydrolyzed.
- (28) de Alwis Watuthanthrige, N.; Dunn, D.; Dolan, M.; Sparks, J. L.; Ye, Z.; Zanjani, M. B.; Konkolewicz, D. Tuning Dual-Dynamic Network Materials through Polymer Architectural Features. *ACS Appl Polym Mater* **2022**, 4 (2), 1475–1486. https://doi.org/10.1021/acsapm.1c01827.
- (29) Guerre, M.; Taplan, C.; Winne, J. M.; du Prez, F. E. Vitrimers: Directing Chemical Reactivity to Control Material Properties. *Chem Sci* **2020**, *11* (19), 4855–4870. https://doi.org/10.1039/dosco1069c.
- (30) Munoz-Robles, B. G.; Kopyeva, I.; DeForest, C. A. Surface Patterning of Hydrogel Biomaterials to Probe and Direct Cell–Matrix Interactions. *Adv Mater Interfaces* **2020**, *7* (21), 2001198. https://doi.org/10.1002/admi.202001198.
- (31) Vedadghavami, A.; Minooei, F.; Mohammadi, M. H.; Khetani, S.; Rezaei Kolahchi, A.; Mashayekhan, S.; Sanati-Nezhad, A. Manufacturing of Hydrogel Biomaterials with Controlled Mechanical Properties for Tissue Engineering Applications. *Acta Biomater* **2017**, 62, 42–63. https://doi.org/10.1016/j.actbio.2017.07.028.
- (32) Amir, F.; Liles, K. P.; Delawder, A. O.; Colley, N. D.; Palmquist, M. S.; Linder, H. R.; Sell, S. A.; Barnes, J. C. Reversible Hydrogel Photopatterning: Spatial and Temporal Control over Gel Mechanical Properties Using Visible Light Photoredox Catalysis. *ACS Appl Mater Interfaces* 2019, 11 (27), 24627–24638. https://doi.org/10.1021/acsami.9bo8853.
- (33) Norris, S. C. P.; Tseng, P.; Kasko, A. M. Direct Gradient Photolithography of Photodegradable Hydrogels with Patterned Stiffness Control with Submicrometer Resolution. *ACS Biomater Sci Eng* **2016**, *2* (8), 1309–1318. https://doi.org/10.1021/acsbiomaterials.6boo237.
- (34) Yuan, Y.; Zhang, H.; Qu, J. Pyridine-Dicarbohydrazone-Based Polyacrylate Hydrogels with Strong Mechanical Property, Tunable/Force-Induced Fluorescence, and Thermal/PH Stimuli Responsiveness. *ACS Appl Polym Mater* **2021**, 3 (9), 4512–4522. https://doi.org/10.1021/acsapm.1c00541.
- (35) Palleau, E.; Morales, D.; Dickey, M. D.; Velev, O. D. Reversible Patterning and Actuation of Hydrogels by Electrically Assisted Ionoprinting. *Nat Commun* **2013**, 4, 2257. https://doi.org/10.1038/ncomms3257.
- (36) Lee, E. H.; Radok, J. R. M. The Contact Problem for Viscoelastic Bodies. *J Appl Mech* **1960**, 27 (3), 438–444. https://doi.org/10.1115/1.3644020.

